

Experimental Evidence for Algebraic Double-Layer Forces

Biljana Stojimirović,¹ Mark Vis,^{2,*} Remco Tuinier,^{2,3} Albert P. Philipse,³ and Gregor Trefalt^{1,†}

¹*Department of Inorganic and Analytical Chemistry, University of Geneva,
Sciences II, 30 Quai Ernest-Ansermet, 1205 Geneva, Switzerland*

²*Laboratory of Physical Chemistry, Faculty of Chemical Engineering
and Chemistry & Institute for Complex Molecular Systems,
Eindhoven University of Technology, The Netherlands*

³*Van 't Hoff Laboratory for Physical and Colloid Chemistry,
Debye Institute for Nanomaterials Science, Utrecht University, The Netherlands*

(Dated: October 2, 2019)

According to textbook wisdom electric double-layer forces decay exponentially with separation distance. Here we present experimental evidence of algebraically decaying double-layer interactions. We show that algebraic interactions arise in both strongly overlapping as well as counterion-only regimes. In both of these cases the disjoining pressure profile assumes an inverse square distance dependence. At small separation distances another algebraic regime is recovered. In this regime the pressure decays as the inverse of separation distance.

I. INTRODUCTION

The repulsion between two charged surfaces immersed in electrolyte solution is usually evaluated under the assumption that electrical double-layers only weakly overlap [1–9]. The implication is that the electrical potential in the mid-plane between the two surfaces is small, which allows for an approximate solution of the Poisson–Boltzmann (PB) equation, that eventually leads to exponentially decaying double-layer repulsions, with a decay distance set by the Debye screening length. Together with van der Waals attractions, exponentially screened repulsions form the classical Derjaguin–Landau–Verwey–Overbeek (DLVO) potential [1–9]. It seems that the weak-overlap requirement has disappeared somewhat from sight, in the sense that textbooks teach exponential screening as a generic feature of double-layer repulsions. However, when charged surfaces immersed in salt solutions approach each other within distances smaller than the Debye length, screening of charges diminishes, or even vanishes, and there is no reason to assume that under this condition exponential decay of double-layer repulsions will remain intact.

For long time, the general opinion about strongly overlapping double-layers in salt solutions was that one has to resort to numerical solutions of the PB-equation to obtain an interaction potential for which there are no simple

expressions [1–9]. Recently, however, it was shown that the weak-potential Debye–Hückel (DH) limit for surfaces far apart, has a pendant limit in the form of a weak electric field for surfaces in close proximity [10]. In the DH case, ions diffuse in a weak but spatially varying potential, whereas in the pendant situation ions roam around in a possibly high but spatially constant electrical potential, a case also known as the Donnan equilibrium [11]. In the zero-field Donnan limit the repulsion between two surfaces in a salt solution can be calculated analytically [10, 26, 27]. The result is an algebraic repulsion where the disjoining pressure decays as an inverse square of separation distance.

Algebraic dependencies are also found in counterion-only systems. These are systems, where charged surfaces are in a bath of only counterions, namely if the surface is negatively charged the adjacent fluid only contains cations. In such systems the counterion concentration profile adjacent to the single charged plate decays algebraically [12–14], in contrast to the system with salt where the counterion profile decays exponentially. The solution for the interaction between two plates immersed in a counterion-only bath was first found by Langmuir [15]. He calculated that in the limit of high charge on the plates the pressure profile also has an algebraic dependence of $1/h^2$.

While reports of experimentally measured exponential double-layer forces are abundant [16–22], there have been only a few articles showing algebraic double-layer forces [23–25] in literature. In all the presented cases these forces were measured in counterion-only regimes. On the

* E-mail: m.vis@tue.nl

† E-mail: gregor.trefalt@unige.ch

other hand algebraic interactions for the strongly overlapping double-layers have only been studied theoretically [10, 26, 27], and experimental instances of algebraic forces between surfaces in 1:1 salt solutions, as far as we know, not been reported yet. The main aim of this paper is to present direct and quantitative evidence for the existence of algebraic interactions between surfaces immersed in simple salt solutions. We also explore different regimes where the algebraic forces are important experimentally.

II. MATERIALS AND METHODS

A. Force Measurements

Forces were measured between spherical silica particles (Bangs Laboratories Inc, USA) with an average reported size of $5.2 \mu\text{m}$. The colloidal probe technique based on atomic force microscopy was used [28–31]. A single silica particle was glued on tip-less cantilever (MicroMasch, Tallin, Estonia) by first immersing the cantilever in a small drop of glue (Araldite 2000+). The substrate was made separately by spreading silica particles on a quartz microscope slide (Plano GmbH, Wetzlar, Germany), which was previously cleaned in piranha solution (3:1 mixture of H_2SO_4 (98%) and H_2O_2 (30%)). Cantilevers with glued-on particles and substrate were both heated at 1200°C for 2 h to achieve firm attachment and removal of the glue. During this sintering process, particles shrink about 15%, so the average diameter is $4.4 \mu\text{m}$ [32]. A root mean square (RMS) roughness of 0.63 nm was measured by AFM imaging in liquid. Solutions were made using KCl (Sigma Aldrich) and Milli-Q water (Millipore). Solutions of pH 10 were made with addition of 1M KOH (Acros Organics), and solutions of pH 3 with 1M HCl (Fisher Scientific). For experiments at pH 5.6 no adjustment was done.

Force measurements were done at room temperature $23 \pm 2^\circ\text{C}$ with a closed loop AFM (MFP-3D, Asylum Research) mounted on an inverted optical microscope (Olympus IX70). Both cantilever and the substrate were cleaned in ethanol and water, and plasma treated for 20 minutes. The substrate with particles was mounted on the fluid cell. The geometry of the experiment is shown in Fig. 1a. The deflection of the cantilever was recorded when the particle on the cantilever was centered above the selected one on the substrate with the precision of about 100 nm. For one pair of particles, the deflection

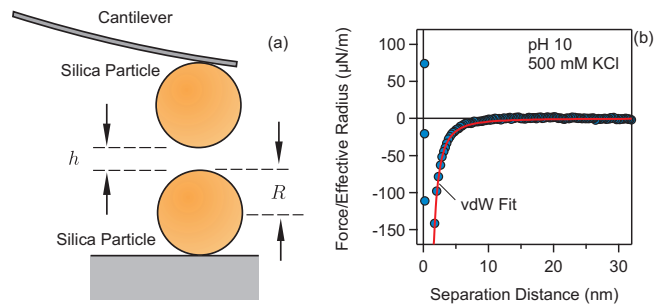


FIG. 1. (a) Schematic representation of colloidal probe experiment. Van der Waals force measured in 500 mM KCl. The extracted Hamaker constant is $H = 2.6 \cdot 10^{-21} \text{ J}$ [32].

is recorded in 150 approach-retract cycles with the cantilever velocity of 400 nm/s. The measurement was done on 3–5 different pairs for each solution concentration. The spring constant of the cantilever was determined by the Sader method [33], and the deflection was converted to force using Hooke's law. The approach part of the recorded curves is averaged and used in analysis.

Our analysis of the experimental forces only focuses on the electrostatic double-layer contribution. However in some cases the van der Waals forces become non-negligible. Therefore the van der Waals force for the present silica–silica system was measured in 500 mM KCl and the respective Hamaker constant was extracted, see Fig. 1b. The van der Waals contribution was then subtracted from all the experimental force profiles. The measured forces $F(h)$ between two spherical particles were then converted to the equivalent disjoining pressure between two plates, $\Pi(h)$, by calculating the derivative of the force versus the separation distance, h , and by applying the Derjaguin approximation

$$\Pi(h) = -\frac{1}{\pi R} \cdot \frac{dF(h)}{dh}, \quad (1)$$

where R is the particle radius.

B. Theory

1. Poisson–Boltzmann Theory

The disjoining pressure between two charged plates is calculated by solving the Poisson–Boltzmann (PB) equation

$$\frac{d^2\Psi(x)}{dx^2} = -\frac{\beta e_0^2}{\varepsilon\varepsilon_0} \sum_i c_i e^{-z_i\Psi(x)}, \quad (2)$$

where $\Psi = \beta e_0 \psi$ is the rescaled dimensionless electrostatic potential, x is the coordinate normal to the plates, c_i is the bulk concentration of ion i , z_i is the valence of ion i , e_0 is the elementary charge, ε_0 is the dielectric permittivity of vacuum, ε is the relative dielectric permittivity of water and $\beta = 1/(k_B T)$ is the inverse thermal energy, where k_B is the Boltzmann constant and T is the temperature. Throughout, $T = 298$ K and $\varepsilon = 80$ are used as appropriate for dilute aqueous solutions. The PB equation is solved numerically with different boundary conditions. One typically assumes a constant charge (CC) or constant potential (CP) on the plates at different distances h , however the charge on the plates can be also regulated upon approach [34–38]. Here we employ constant regulation approximation, where we introduce the regulation parameter p , which interpolates between CP ($p = 0$) and CC ($p = 1$) boundary conditions [35, 39]. The solution of the PB equation yields the potential profile $\psi(x)$ between two charged plates positioned at $x = -h/2$ and $x = +h/2$. The potential at the mid-plane, $\psi_M = \psi(0)$, then permits to calculate the disjoining pressure

$$\Pi(h) = k_B T \sum_i c_i \left(e^{-z_i \Psi_M(h)} - 1 \right), \quad (3)$$

where h is the distance between the plates.

Further details of the implementation of the full PB theory including constant charge regulation model are given in Ref. 32.

2. Strongly Overlapping Double-Layers

For strongly overlapping double-layers analytical approximations of the PB equation can be found as was demonstrated recently [10, 26, 27]. These approximations are applicable for symmetric $z : z$ electrolytes and here we will focus only on the 1:1 case. For 1:1 electrolytes, the disjoining pressure can be calculated by simplifying Eq. (3)

$$\Pi = 2k_B T c_s [\cosh(\Psi_M) - 1]. \quad (4)$$

For strongly overlapping double-layers, the electrical potential between the plates deviates only little from its average value, i.e. the electric field in the gap is approximately zero. The mid-plane potential in the equation above can be then be replaced by a constant $\Psi_M = \overline{\Psi}$, where $\overline{\Psi}$ turns out to be the dimensionless Donnan potential. The value of the Donnan potential can be determined from the electro-neutrality condition for the two

plates and the intermediate salt solution

$$\frac{\overline{c}_+ - \overline{c}_-}{2c_s} = \frac{\lambda}{h}, \quad (5)$$

where \overline{c}_+ and \overline{c}_- refer to the cation and anion number concentrations between the plates, respectively. We have introduced characteristic length λ defined as

$$\lambda = \frac{\sigma}{c_s e_0} = \frac{4}{\kappa^2 \ell_{GC}}, \quad (6)$$

where σ is the surface charge density of the plates and $\kappa = \sqrt{8\pi\ell_B c_s}$ is the inverse Debye length, with $\ell_B = \beta e_0^2 / (4\pi\varepsilon\varepsilon_0)$ the Bjerrum length, and

$$\ell_{GC} = \frac{e_0}{2\pi\ell_B \sigma} \quad (7)$$

is the Gouy–Chapman length.

By combining Eq. (5) with the Boltzmann equilibrium for exchanging ions between bulk and the gap

$$\overline{c}_\pm = c_s e^{\mp\overline{\Psi}}, \quad (8)$$

we can calculate the value of the Donnan potential

$$\overline{\Psi} = -\sinh^{-1} \left(\frac{\lambda}{h} \right). \quad (9)$$

The zero-field pressure can be finally calculated by inserting Eq. (9) into Eq. (4)

$$\Pi = 2k_B T c_s \left(\sqrt{1 + \left(\frac{\lambda}{h} \right)^2} - 1 \right). \quad (10)$$

For $\lambda/h \ll 1$, i.e. large separation and low surface charge, the above equation reduces to

$$\Pi = k_B T c_s \left(\frac{\lambda}{h} \right)^2. \quad (11)$$

The pressure for strongly overlapping double-layers therefore decays algebraically $\Pi \propto 1/h^2$. Another algebraic dependence is recovered at small separations

$$\Pi = 2k_B T c_s \cdot \frac{\lambda}{h} = \frac{2\sigma k_B T}{e_0} \cdot \frac{1}{h}. \quad (12)$$

This latter equation is similar to the ideal-gas equation of state, $P = Nk_B T/V$, and we will refer to it as the ideal-gas equation [14].

The disjoining pressure in the zero-field approximation is derived here for plates with constant charge densities. When one includes charge regulation effects, the resulting pressure decay is not affected, but only the amplitude weakens [26, 27]. It has been also shown that the Donnan potential in Eq. (9) results from the asymptotic solution of the PB-equation for vanishing electric field [10].

3. Counterion-Only Double-Layers

In the counterion only case the disjoining pressure also decays algebraically [15, 24, 40]. Here the only ionic species are the counterions to the surfaces. If one assumes a positively charged surface and anions as counterions, the PB equation reduces to

$$\frac{d^2\Psi(x)}{dx^2} = \frac{\beta e_0^2 c_-}{\varepsilon \varepsilon_0} e^{\Psi(x)}. \quad (13)$$

This equation can be solved analytically for two charged plates and the resulting potential profile is

$$\Psi(x) = \Psi_M - \ln \left[\cos^2 \left(\frac{x\gamma}{\ell_{GC}} \right) \right], \quad (14)$$

where $\gamma = e^{\Psi_M - \Psi_D}$, Ψ_D being the diffuse-layer potential at the isolated plate surface. The disjoining pressure in this case is equal to the pressure between the plates, since the bulk pressure vanishes without salt and is calculated by using Eq. (14)

$$\Pi = k_B T c_- e^{\Psi_M} = \frac{2\varepsilon\varepsilon_0}{\beta^2 e_0^2 \ell_{GC}^2} \gamma^2. \quad (15)$$

The equation above shows that γ^2 is actually the rescaled pressure. For the constant charge boundary conditions the relation between the separation distance and pressure becomes [24]

$$h = \frac{2\ell_{GC}}{\gamma} \arctan(\gamma^{-1}). \quad (16)$$

At large separation distances the pressure tends to zero and one can approximate $\arctan(x) \approx \frac{\pi}{2}$. With this we can rewrite the equation above as

$$\Pi = \frac{\pi}{2\beta\ell_B} \cdot \frac{1}{h^2}. \quad (17)$$

Here, the decay of the pressure is also algebraic. This equation was first derived by Langmuir [15] and we will refer to it as the Langmuir equation. Note that the Langmuir equation features the same $1/h^2$ dependence as the zero-field result given in Eq. (11), albeit the pre-factor and physical origin are different.

In the opposite limit, *i.e.* short separation distances, where $\arctan(x) \approx x$, Eq. (16) reduces to the ideal-gas equation shown in Eq. (12). Therefore both the counterion-only and zero-field approximation lead to the same result for small separation distances. The ideal-gas equation can be understood for the counterion-only case in the following way. When plates come sufficiently close

together, all the coions are expelled and only counterions remain. Due to charge neutrality, the number of counterions in the gap must be equal to the number of charges on the plates. The distance between the plates and the area of the plates therefore determine the concentration of the ions in the gap as $c = 2\sigma/(e_0 h)$; multiplying this concentration by $k_B T$ leads to the disjoining pressure in Eq. (12).

For the case of asymmetric $z : 1$ salts, where z is the valence of the coion, the multivalent coions get expelled from the gap between the charged plates upon approach [24, 32]. This situation results in a counterion-only system, however the salt is still present in the bulk. We can correct the Langmuir pressure for the bulk contribution. If we add an additional term in the $\arctan(x) \approx \frac{\pi}{2} - \frac{1}{x}$ expansion we arrive at [25]

$$\Pi = \frac{\pi}{2\beta\ell_B} \cdot \frac{1}{(h + 2\ell_{GC})^2} - \frac{(z+1)c_s}{\beta}. \quad (18)$$

We refer to this approximation as the corrected Langmuir equation.

III. RESULTS AND DISCUSSION

We use the colloidal probe technique based on AFM microscopy to experimentally study algebraic double-layer forces between colloidal particles. Specifically, we measure the double-layer interactions between micron-sized silica particles in the presence of KCl at different pH. We further analyze the forces in $K_4Fe(CN)_6$ to show experimental evidence of counterion-only induced algebraic double-layer interactions.

First the van der Waals forces are subtracted from all the experimentally measured forces, which yields only the double-layer contribution to the force profile. The resulting double-layer forces are then converted to disjoining pressures between plates by calculating the derivative of the force versus the separation distance. These experimental pressure profiles are then fitted with the full PB theory and the silica surface properties are extracted from the fits. Note that the concentrations are fixed to nominal values during fitting. The diffuse-layer potentials and regulation parameters for silica particles extracted from this fitting procedure are shown in Fig. 2. As expected for silica surfaces in aqueous solutions, the double-layer potentials are increasing with increasing salt concentration due to electrostatic screening. The particles acquire most negative charge at pH 10, where the

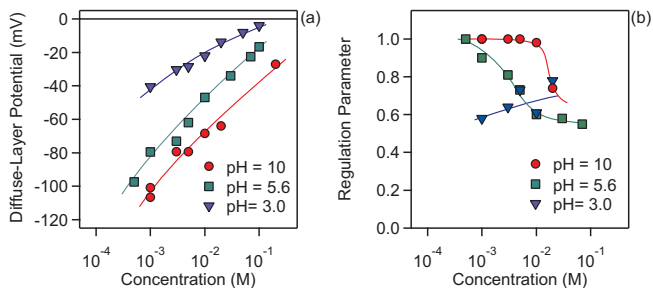


FIG. 2. (a) Diffuse-layer potential and (b) regulation parameter as a function of KCl concentration for different pH conditions. These parameters were extracted by fitting experimental force data with full PB theory.

fraction of charged silanol groups is the highest. On the other hand, regulation parameters are decreasing with increasing concentration at pH 10 and pH 5.6, while they are modestly increasing at pH 3. These observations are consistent with earlier reports, where a similar decrease in the regulation parameters was reported for pH 10, while at pH 4 the regulation parameters were constant [18]. Note that regulation parameter of 1 represents constant charge conditions (CC), while at constant potential (CP) conditions the regulation parameter is 0 and the surface charge varies strongly when the two surfaces approach each other. Therefore at high pH and low concentration the silica particles behave as CC surfaces, while they regulate more strongly at low pH and high salt concentrations. Surface properties of silica reported in Fig. 2 are not the main interest of the present paper, but they are used to determine which asymptotic regimes are applicable at certain solution conditions. The double-layer potentials are further converted by employing the Grahm equation to surface charge density and used to calculate characteristic length scales, such as Gouy–Chapman length.

The main focus of the present paper is the analysis of the asymptotic laws in the experimental double-layer interactions. In Fig. 3, an example of disjoining pressure measured at pH 10 and 3 mM KCl is shown. The exponential function $e^{-\kappa h}$, and two algebraic functions $1/h$ and $1/h^2$ are also shown in the figure. Note that the amplitudes of these general functions are adjusted to fit the experimental data. The data is shown in log–lin and log–log representations for clarity. This simple comparison reveals that the experimental data has an exponential dependence only at separation distances above ~ 15 nm, where the double-layers from the two surfaces are only weakly overlapping. At intermediate distances between

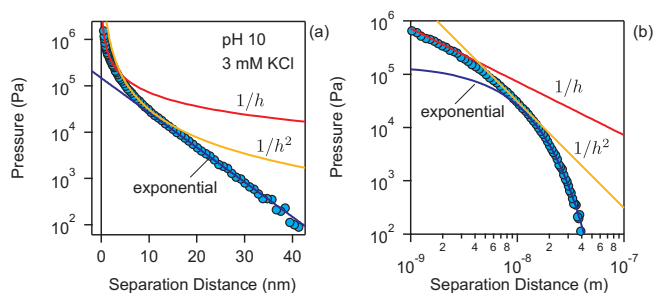


FIG. 3. Comparison of (a) log–lin and (b) log–log representations for disjoining pressure between two silica particles measured at pH 10 and 3 mM KCl. The algebraic $1/h$ and $1/h^2$ as well as exponential curves are also shown.

5 and 15 nm the double-layers overlap strongly and the $1/h^2$ dependence becomes applicable, while at distances below 5 nm the pressure decreases as $1/h$.

Let us now have a more detailed look at the applicability of the approximations introduced in the theory section. First we will focus on strongly overlapping double-layers, where the zero-field approximation shown in Eq. (10) is expected. In Fig. 4, the disjoining pressures for different pH conditions and different salt levels are shown. Note that pressures are normalized to bulk osmotic pressure while distance is normalized with Debye length. Together with experimental data we plot the algebraic zero-field approximations shown in Eqs. (10), (11), and (12). We further denote the value of $\kappa\lambda$ in the sub-figures, which represents the value of the characteristic length in comparison to the Debye length and permits the evaluation of the accuracy of the zero-field approximations [10].

In the top row of Fig. 4, the data for pH 3 are shown. At pH 3 the silica surface exhibits the lowest surface charge and the regulation parameter is around $1/2$ as evident from Fig. 2. By comparing the experimental pressures to the calculated ones, one can deduce that the double-layers start to overlap strongly at distances shorter than about $2-3 \kappa h$ and the zero-field approximation Eq. (10) becomes accurate. The simplified inverse square separation dependence $1/h^2$ shown in Eq. (11) represents a good approximation at intermediate separations at about $\kappa h \approx 1$ and gets more accurate at higher salt concentrations. The accuracy of the $1/h^2$ dependence, Eq. (11), is good at $\kappa\lambda \leq 1$, as discussed earlier [10], therefore one needs to go to high salt concentrations and low pH for it to become applicable. Furthermore for pH 3 solutions the ideal-gas equation is not accurate since the surfaces strongly regulate and the ideal-gas

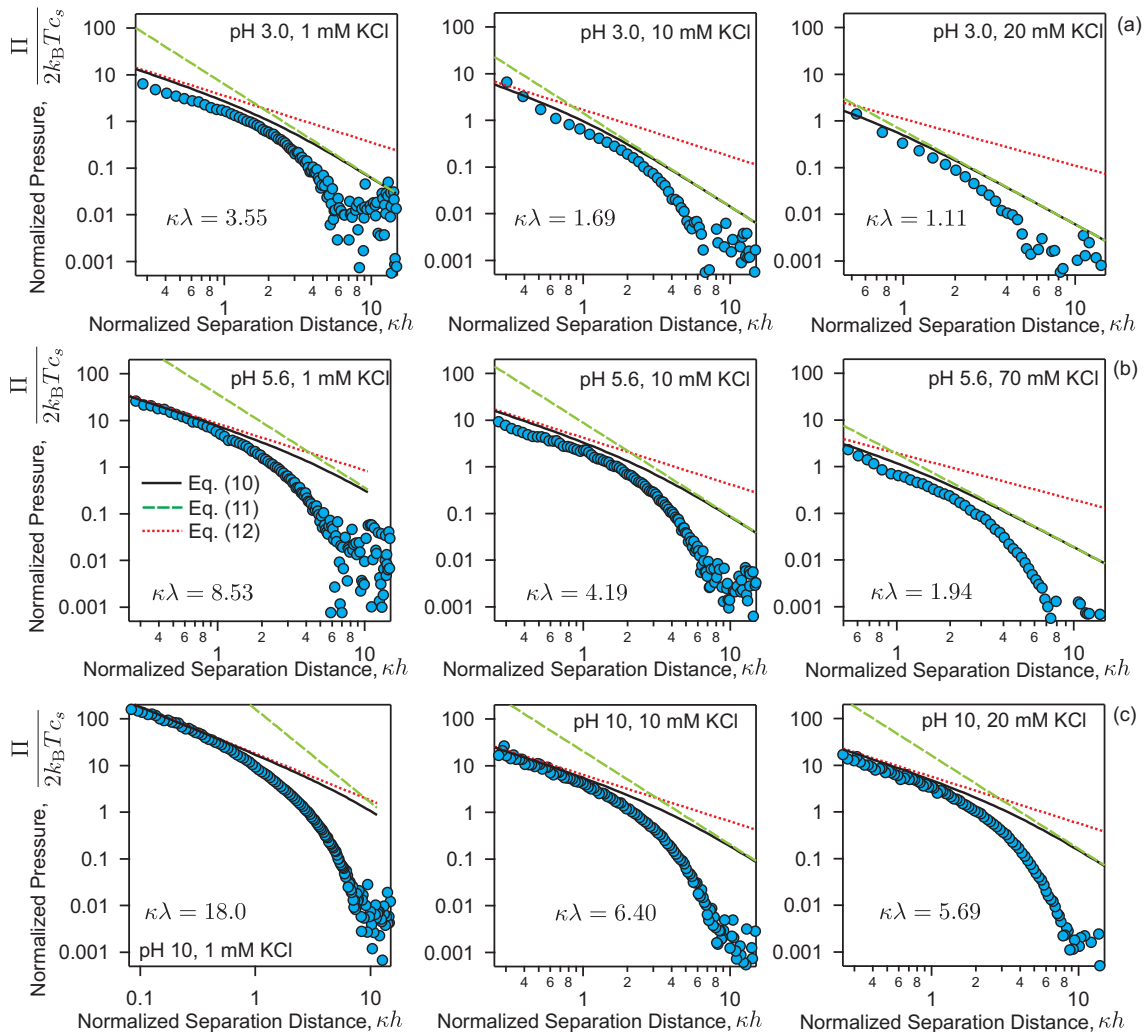


FIG. 4. Zero-Field theory compared to experimental disjoining pressures measured at (a) pH 3.0, (b) pH 5.6, and (c) pH 10. Different columns present different salt levels. Experimental data is shown with symbols, while full, dashed, and dotted lines represent Eqs. (10), (11), and (12), respectively.

equation is derived for constant charge surfaces.

At intermediate pH values of 5.6 shown in Fig. 4b, the zero-field approximation works the best at low concentration and small separation distances. The simple $1/h^2$ dependence, Eq. (11), gets again more accurate at higher concentrations, but it is less accurate compared to pH 3 case, because the magnitude of the charge on silica is higher at higher pH. The ideal-gas equation works best at low concentrations, since in this case the regulation parameter is close to 1 and the surface has approximately constant charge.

When pH is increased to 10 (Fig. 4c), the $1/h^2$ approximation gets even less accurate since the magnitude of the charge again increases and consequently $\kappa\lambda$ further increases. On the other hand, the particles now follow the

CC behavior and the ideal-gas $1/h$ dependence is highly accurate at small separations.

Looking at all the sub-figures in Fig. 4, one can deduce that the simple algebraic $1/h^2$ dependence from Eq. (11) accurately describes silica-silica interactions at intermediate separation distances at low pH and high salt concentrations, where $\kappa\lambda \leq 1$ is satisfied. The ideal-gas relation Eq. (12) is accurate at small separation distances, typically below $\kappa h \leq 1$, and at low concentrations and high pH, where the regulation parameter is close to 1. Therefore experimental conditions where double-layers overlap strongly and algebraic interactions are present are readily reached in 1:1 electrolytes.

Let us now address the comparison of the zero-field approximation Eq. (11) with Langmuir expression,

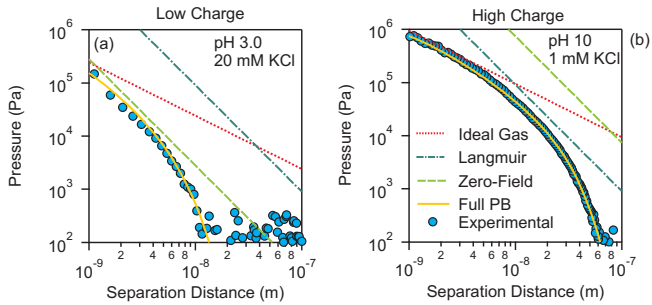


FIG. 5. Comparison of zero-field and Langmuir approximation for the (a) low charge and (b) high charge experimental cases.

Eq. (17). While the former is valid for strongly overlapping double-layers in 1:1 electrolyte, the latter is derived for counterion-only double-layers. Both of these approximations are valid at the intermediate separation distances and they both feature an inverse square distance dependence $1/h^2$. The difference between them is in the amplitude *i.e.* strength of the interaction. In Fig. 5 a comparison of the algebraic interactions is made for weakly and highly charged systems, respectively. The left sub-figure shows the disjoining pressure at pH 3 and 20 mM KCl, while the right subfigure shows the interaction at pH 10 and 1 mM KCl. In both cases the full PB is used to fit the experimental data, and the PB theory perfectly describes the data in the whole distance range. At pH 10 the experimental pressure follows the $1/h$ ideal-gas dependence at small separations, while at pH 3 this regime is not recovered due to stronger charge regulation of silica surfaces at this condition. The zero-field $1/h^2$ dependence, Eq. (11), predicts the behavior rather well at pH 3, while it largely overestimates the repulsion at pH 10. The opposite is true for the Langmuir equation, which works better at pH 10 and it overestimates the pressure at pH 3. These results are consistent with the range of validity for both models. While the zero-field approximation is valid for weakly charged surfaces, the Langmuir equation is applicable for highly charged surfaces [10, 14, 26].

Another important experimental case where algebraic interactions are important is the multivalent coion case. In these systems, the multivalent ions have the same sign of charge as the surface. When two charged plates approach each other in these salts, at a certain distance, the multivalent coions are expelled from the gap between the charged plates [24, 25, 32]. After the expulsion of the coions, the systems behaves as counterion-

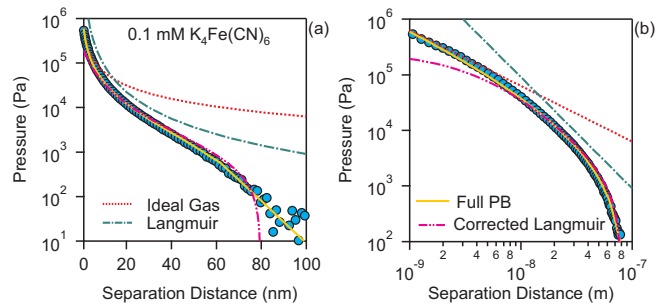


FIG. 6. Experimentally measured disjoining pressure in the presence of 0.1 mM $K_4Fe(CN)_6$ at pH 10. (a) Log–lin and (b) lin–lin representations of experimental data. The full PB model for the mixture of 1:z and 1:1 electrolyte is shown together with ideal-gas (12), Langmuir (17), and corrected Langmuir (18) approximations.

only and the pressure decays algebraically. An example of such interactions between two silica colloids in the presence of $K_4Fe(CN)_6$ salt at pH 10 is shown in Fig. 6. Again the disjoining pressure profile can be perfectly described with the full PB model. At separation distances above ~ 80 nm, the pressure decays exponentially, and here both coions and counterions are still present in the gap. At separations below ~ 70 nm the four-valent $[Fe(CN)_6]^{4-}$ ions get expelled from the gap, only K^+ ions are left, and the system transitions into counterion-only regime. Here the pressure decays algebraically. The Langmuir equation captures this $1/h^2$ dependence, but it overestimates the magnitude of the force. If one corrects the Langmuir equation by accounting for the ions in the bulk and expanding the approximation with one more term, the resulting Eq. (18) describes the data very well in the separation range from 5 to 80 nm. At distances below 10 nm, the ideal-gas equation offers a quantitative description of the data. In the multivalent coion systems where the pressure decays algebraically, the counterion-only regime is typically important in very wide separation range, and the *textbook* exponential double-layer forces become evident only at very large distances where they are weak. In the presence of multivalent coions, the aggregation of colloids is also driven by the algebraic forces and leads to the *inverse* Schulze-Hardy rule reported recently by some of us [41]. Similar algebraically decaying interactions were recently measured in the presence of like-charged polyelectrolytes [25] and between stacked charged bilayers [42]. In the case of polyelectrolytes, the transition between algebraic and exponential regimes is even more abrupt, due to the larger charge of the poly-

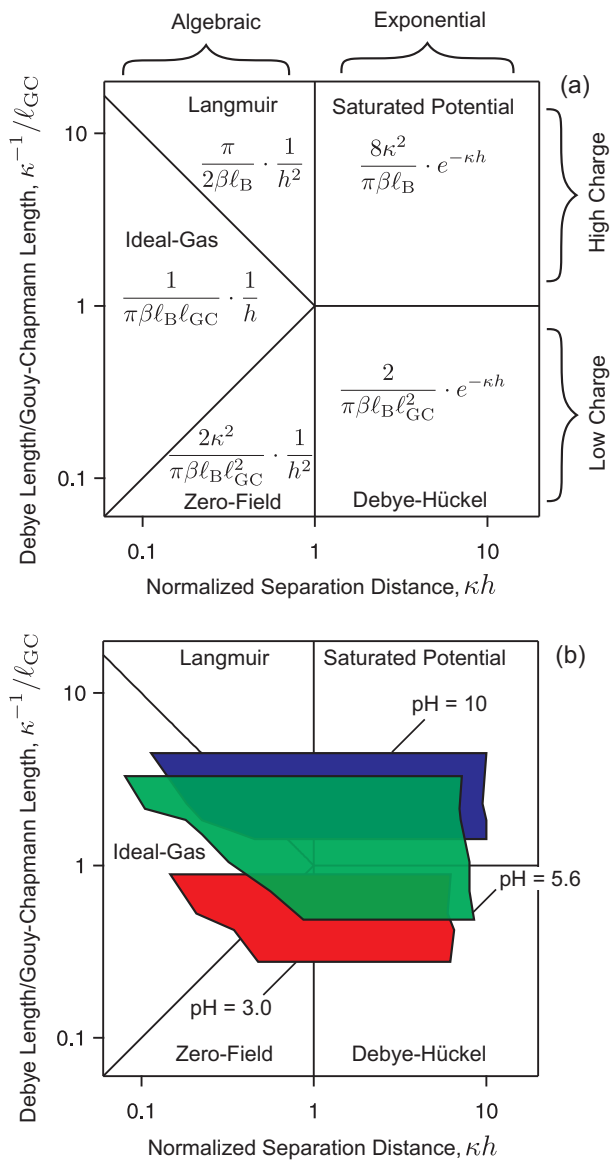


FIG. 7. Approximation validity map for interaction of charged plates across symmetric electrolytes. (a) Map showing the relevant regimes with equations. Experimentally accessible ranges for silica in KCl solutions at (b) pH 3.0, (c) pH 5.6, and (d) pH 10.

electrolytes as compared to multivalent coions.

Let us finally give an overview at what conditions the presented approximations are valid for symmetric electrolytes. Approximation validity maps are shown in Fig. 7. Similar map was presented in [14] and here we add the ranges where experimental interactions between silica colloids were measured. In Fig. 7a, we present the areas of validity for different approximations with the corresponding equations. The y -axis represents Debye length divided by the Gouy–Chapman and the values

are increasing with increasing surface charge density and decreasing salt concentration. On the x -axis, the separation distance relative to the Debye length is given. The map can be divided into 5 regions. Note that in reality the borders between the regions are not sharp lines as drawn here, but are more fuzzy. The map can be divided into small separation ($\kappa h < 1$) and large separation distances ($\kappa h > 1$), where algebraic and exponential approximations are dominant, respectively. At very small distances and intermediate charge, the ideal-gas equation (12) is applicable. Note that the ideal-gas law is only valid for constant charge surfaces. At intermediate distances and for highly charged particles, the Langmuir equation Eq. (17) is accurate. The range of validity can be extended to lower charges by using the corrected Langmuir approximation Eq. (18). At low charge and intermediate distance, the zero-field approximation Eq. (11) is applicable. At distances $\kappa h > 1$, the pressure profiles become exponential. Here we can approximate the low charged case with the Debye–Hückel superposition approximation, while for the highly charged surfaces one has to replace the diffuse-layer potential in the Debye–Hückel approximation with the effective saturated potential [9].

In Fig. 7b we highlight the regions where the measurements between silica colloids were done in the present paper. The position of the range, where the force measurements are located in the map, changes depending on the salt concentration and pH of the solutions. The AFM measurements can be done reliably down to ~ 1 nm separation distances, while the limit for large separations depends on the magnitude of the force, which in turn depends on the charge of the surfaces. Therefore, the range where the measurements can be performed is moving down and to the right with increasing concentration, by increasing κ . On the other hand, increasing the pH shifts the ranges up due to increasing magnitude of the surface charge, which decreases ℓ_{GC} . For all the pH conditions studied, the ideal-gas law is retrieved at low concentrations and sufficiently small separations for CC surfaces, which is consistent with the data presented in Fig. 4. For pH 10 and pH 3, the experimental data falls into the high and low charge regimes, respectively. Therefore, the Langmuir approximation is most accurate at pH 10 for intermediate distances, while the zero-field approximation works best at pH 3. At pH 5.6 none of the $1/h^2$ approximations is very accurate since the surface charge density is in this case in the intermediate

regime.

IV. CONCLUSIONS

Algebraic double-layer interactions have been demonstrated experimentally for simple 1:1 salts. This type of force is also present for systems containing highly-charged coions, where they come from the counterion-only dominated regime. Both strongly overlapping double-layer (zero-field) and counterion-only (Langmuir) regimes recover the inverse square distance dependence of disjoining pressures albeit with different pre-factor. The former is applicable for weakly charged surfaces, the latter for highly charged surfaces. Independent of the surface charge, at very small separation distances the $1/h$ ideal-gas limit is recovered for non-regulating constant charge surfaces. In the other limit, at large separation distances, the Debye–Hückel dependence is observed and

pressures follow the textbook exponential profile. The textbook wisdom is therefore correct at large separations, but at small separations the profiles are algebraic. The latter regime is also important in experimental situations, for example for colloidal aggregation in the presence of multivalent coions, or for systems containing like-charged polyelectrolytes.

ACKNOWLEDGMENTS

This research was supported by the Swiss National Science Foundation through grant 162420 and the University of Geneva. The authors are thankful to Michal Borkovec for providing access to the instruments in his laboratory and to Plinio Maroni for the help with AFM measurements. MV acknowledges the Netherlands Organisation for Scientific Research (NWO) for a Veni grant (no. 722.017.005).

-
- [1] B. Derjaguin, *Trans. Faraday Soc.* **10**, 333 (1940).
 [2] B. Derjaguin and L. D. Landau, *Acta Phys Chim* **14**, 633 (1941).
 [3] E. J. W. Verwey and J. T. G. Overbeek, *Theory of Stability of Lyophobic Colloids* (Elsevier, Amsterdam, 1948).
 [4] H. R. Kruyt, G. H. Jonker, and J. T. G. Overbeek, *Colloid Science, Edited by H.R. Kruyt. [Contributors: G.H. Jonker and J. Th. G. Overbeek. English Translation by L.C. Jackson.] Vol. I. Irreversible Systems* (Elsevier, 1952).
 [5] D. F. Evans and H. Wennerstrom, *The Colloidal Domain* (John Wiley, New York, 1999).
 [6] W. B. Russel, D. A. Saville, and W. R. Schowalter, *Colloidal Dispersions* (Cambridge University Press, Cambridge, 1989).
 [7] J. Lyklema, *Fundamentals of Interface and Colloid Science: Particulate Colloids* (Elsevier, 2005).
 [8] J. Israelachvili, *Intermolecular and Surface Forces*, 3rd ed. (Academic Press, London, 2011).
 [9] M. Elimelech, J. Gregory, and X. Jia, *Particle Deposition and Aggregation: Measurement, Modelling and Simulation* (Butterworth-Heinemann, 2013).
 [10] A. P. Philipse, B. W. M. Kuipers, and A. Vrij, *Langmuir* **29**, 2859 (2013).
 [11] A. Philipse and A. Vrij, *J. Phys.: Condens. Matter* **23**, 194106 (2011).
 [12] M. Gouy, *J. Phys. Theor. Appl.* **9**, 457 (1910).
 [13] D. L. Chapman, *Philos. Mag.* **25**, 475 (1913).
 [14] T. Markovich, D. Andelman, and R. Podgornik, *ArXiv160309451 Cond-Mat* (2016), arXiv:1603.09451 [cond-mat].
 [15] I. Langmuir, *J. Chem. Phys.* **6**, 873 (1938).
 [16] S. D. Finlayson and P. Bartlett, *J. Chem. Phys.* **145**, 034905 (2016).
 [17] S. K. Sainis, J. W. Merrill, and E. R. Dufresne, *Langmuir* **24**, 13334 (2008).
 [18] A. M. Smith, P. Maroni, M. Borkovec, and G. Trefalt, *Colloids Interfaces* **2**, 65 (2018).
 [19] J. N. Israelachvili and G. E. Adams, *J. Chem. Soc.-Faraday Trans. I* **74**, 975 (1978).
 [20] D. C. Prieve, *Adv. Colloid Interface Sci.* **82**, 93 (1999).
 [21] I. Popa, P. Sinha, M. Finessi, P. Maroni, G. Papastavrou, and M. Borkovec, *Phys Rev Lett* **104**, 228301 (2010).
 [22] A. M. Smith, A. A. Lee, and S. Perkin, *J. Phys. Chem. Lett.* **7**, 2157 (2016).
 [23] W. H. Briscoe and R. G. Horn, *Langmuir* **18**, 3945 (2002).
 [24] F. J. M. Montes Ruiz-Cabello, M. Moazzami-Gudarzi, M. Elzbieciak-Wodka, P. Maroni, C. Labbez, M. Borkovec, and G. Trefalt, *Soft Matter* **11**, 1562 (2015).
 [25] M. Moazzami-Gudarzi, T. Kremer, V. Valmacco, P. Maroni, M. Borkovec, and G. Trefalt, *Phys. Rev. Lett.* **117**, 088001 (2016).
 [26] A. P. Philipse, R. Tuinier, B. W. M. Kuipers, A. Vrij, and M. Vis, *Colloid and Interface Science Communications* **21**, 10 (2017).
 [27] M. Vis, R. Tuinier, B. W. M. Kuipers, A. Vrij, and A. P. Philipse, *Soft Matter* **14**, 4702 (2018).
 [28] M. Borkovec, I. Szilagy, I. Popa, M. Finessi, P. Sinha, P. Maroni, and G. Papastavrou, *Adv. Colloid Interface*

- Sci. **179-182**, 85 (2012).
- [29] H. J. Butt, B. Cappella, and M. Kappl, *Surf. Sci. Rep.* **59**, 1 (2005).
- [30] H. J. Butt, *Biophys. J.* **60**, 1438 (1991).
- [31] W. A. Ducker, T. J. Senden, and R. M. Pashley, *Nature* **353**, 239 (1991).
- [32] B. Uzelac, V. Valmacco, and G. Trefalt, *Soft Matter* **13**, 5741 (2017).
- [33] J. E. Sader, J. W. M. Chon, and P. Mulvaney, *Rev. Sci. Instrum.* **70**, 3967 (1999).
- [34] Y. Avni, D. Andelman, and R. Podgornik, *Current Opinion in Electrochemistry* **13**, 70 (2019).
- [35] S. H. Behrens and M. Borkovec, *J. Chem. Phys.* **111**, 382 (1999).
- [36] J. G. Kirkwood and J. B. Shumaker, *Proc. Natl. Acad. Sci. U. S. A.* **38**, 863 (1952).
- [37] T. Markovich, D. Andelman, and R. Podgornik, *EPL* **113**, 26004 (2016).
- [38] N. Adžić and R. Podgornik, *Eur. Phys. J. E* **37**, 49 (2014).
- [39] G. Trefalt, S. H. Behrens, and M. Borkovec, *Langmuir* **32**, 380 (2016).
- [40] W. H. Briscoe and P. Attard, *J. Chem. Phys.* **117**, 5452 (2002).
- [41] T. Cao, I. Szilagyi, T. Oncsik, M. Borkovec, and G. Trefalt, *Langmuir* **31**, 6610 (2015).
- [42] M. Hishida, Y. Nomura, R. Akiyama, Y. Yamamura, and K. Saito, *Phys. Rev. E* **96**, 040601 (2017).